

AIRSAR VIEWS OF AEOLIAN TERRAIN

Dan G. Blumberg and Ronald Greeley

Department of Geology

Arizona State University

Tempe Az. 85287-1404

1. OVERVIEW

Remote sensing observations of terrestrial dune morphologies provide information on sand transport, climate, and soil processes associated with aeolian processes. In this study AIRSAR images of the Stovepipe Wells Dune Field, California, were examined to assess the degree to which dune types can be determined from radar images and the factors leading to the formation of four different dune types in one locality. The images were acquired during the Geologic Remote Sensing Field Experiment (GRSFE; Evans et al., in press) and later. These images provide a unique opportunity to enhance the knowledge of how radar images allow discrimination of dune forms.

2. RADAR DATA

Radar images were obtained in September 1989 and May 1992 by the Jet Propulsion Laboratory synthetic aperture radar - AIRSAR. The images have a resolution of ~12 m per pixel and are acquired in C-band ($\lambda = 5.6$ cm), L-band ($\lambda = 24$ cm), and P-band ($\lambda = 67$ cm). All images were calibrated using POLCAL (van Zyl et al., 1992). Although the entire Stokes matrix is saved for the images and any polarization can be extracted, only the co- and cross-polarized data were extracted (HH; VV; HV-VH). Figure 1 (See Slide 12) shows an image of the total power return at Stovepipe Wells for C, L, and P-band in HH polarization.

The illumination was from the west and the flight direction from north to south. The look angle was 45° .

3. OBSERVATIONS

The Stovepipe Wells Dune field covers an area of ~ 100 km² in northern Death Valley, California ($117^\circ 06' W$ $36^\circ 39' N$). Four dune types, each characteristic of a different wind regime, occur at Stovepipe Wells: reverse dunes, star dunes, transverse, and linear dunes. In addition to dunes, C-band images reveal a mantle of sand around the dune field. Field observations show that local saline crusts in the sand mantle cause microscale roughness variations that give a mottled radar backscatter cross section that is prominent in C-band but less pronounced in P and L-bands.

3.1 Reverse dunes

The reverse dunes are low (typically < 5 m high), formed by temporal reversals of the wind direction through the valley (N - S). The reverse dunes are observed in the radar images as dark and bright linear features on the northeast part of the field. The dunes appear as dark narrow streaks aligned east-west with bright interdune regions. The low reverse dunes are not seen in P-band, but are visible in C-band. They are best observed in the H-H images, and not seen in the cross-polarized image.

3.2 Star dunes

The star dunes have a maximum height of 40 m above the surrounding surface and are formed by polymodal winds transporting sand to the center of the dune field. Star dunes have at least three flanks which create a trihedral corner reflector effect in radar images. The result is an extremely bright speckle from the interdune zone facing the antenna. These dunes are easily recognized in AIRSAR images of Stovepipe Wells because of the quasi-speckular return from the corner between the dune flanks. The quasi-speckular signature is visible in all wavelengths.

3.3 Transverse Dunes

Transverse dunes are found in the northern part of the dune field. These are formed by unimodal winds blowing from the north. The winds from the south (that are partly responsible for the reverse dunes) are blocked by a mountain and by the large star dunes. The transverse dunes appear in the radar images as alternating bright and dark stripes. These dunes exhibit bright lee slopes and dark narrow stoss slopes. Transverse dunes are visible in all wavelengths but are not seen in the cross-polarized data.

3.4 Linear dunes

In the west part of the dune field there is a set of linear dunes which are formed by bi-directional winds coming from the northeast and southeast. Blom and Elachi (1981) state that the interdune spacing needs to be at least 3 to 4 picture elements wide to be able to detect linear dunes. The interdunal spacing of these dunes is greater than 4 pixels. In the 1992 image these dunes appear as narrow reflective streaks. Because the linear dunes are in the very near range, their form is more difficult to resolve in this image than other dune types.

3.5 Vegetated dunes

Very sparse vegetation exists at the Stovepipe Wells Dune Field. The vegetation is primarily in clusters over the sand mantle and in an area where the dune forms change from reverse to star dunes. While vegetation can be seen in all images it is most pronounced in the cross-polarized images. Comparison of the vegetation in the radar images to aerial photographs from 1948 do not show any spatial change in the vegetation pattern.

4. Conclusion

The Stovepipe Wells Dune Field provides a unique opportunity to observe several dune forms in one scene. These forms include reverse dunes, star dunes, transverse, and linear dunes. A sand mantle surrounds the dune field and can also be observed in the radar image. Dune types were discriminated best in co-polarized channels.

Three major wind directions are responsible for the various dune forms. Wind from the north and south are responsible for the reverse dunes, winds from north the for the transverse dunes, and the north - south and westerly winds form the star dunes. The winds also reflect the topographic configuration of this part of the valley.

Vegetation over the dunes was most pronounced in the cross-polarized images. Lancaster et al. (1992) finds that cross-polarized images are most useful in differentiating active from inactive dunes. This is because the vegetation backscatter signature is present over inactive dunes.

Future studies should include multiple look and incidence angles to determine if the dune forms can still be seen at other angles.

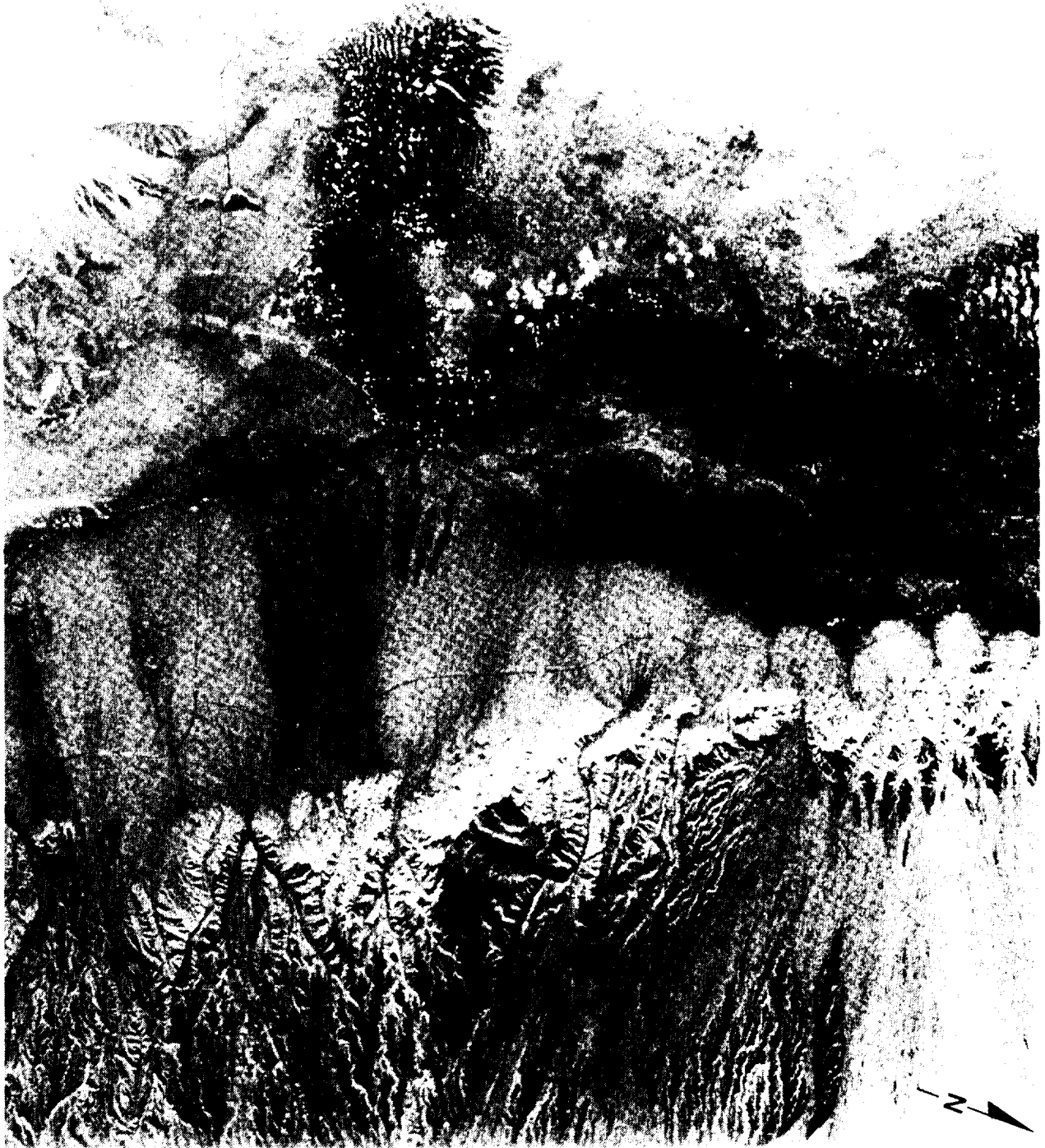


Figure 1. AIRSAR image of Stovepipe Wells Dune Field, Death Valley, California. The image shows total power for C, L, and P-bands

References cited:

Blom R. and C. Elachi, 1987, "Spaceborne and Airborne Imaging Radar Observations of Sand Dunes", *J. Geophys. Res.*, 86 (B4), 3061-3073.

Evans D.L., T.G. Farr, M. Vogt, C. Bruegge, J. Conel, R.E. Arvidson, S. Petroy, J.J. Plaut, M. Dale-Bannister, E. Guinness, R. Greeley, N. Lancaster, L. Gaddis, J. Garvin, D. Deering, J. R. Irons, F. Kruse, D. J. Harding, submitted, "The Geologic Remote Sensing Field Experiment", *IEEE Transaction of Geoscience and Remote Sensing*.

Lancaster N., L. Gaddis, and R. Greeley, 1992, "New Airborne Imaging Radar Observations of Sand Dunes: Kelso Dunes", California, *Remote Sens. Environ.*, 39, pp. 233-238.

van Zyl J.J., C.F. Burnette, H.A. Zebker, A. Freeman, J. Holt, 1992, *Polcal Users Manual*, JPL D-7715 version. 4.0., pp. 48.